

# SINTERING OF 6H( $\alpha$ )-SiC AND 3C( $\beta$ )-SiC COMMERCIAL POWDERS WITH B<sub>4</sub>C AND C ADDITIVES

Yoshimura, H.N.(1); Zhou, Y.(2); Tanaka, H.(3)

(1) Instituto de Pesquisas Tecnológicas do Estado de São Paulo S.A. - IPT  
Divisão de Química - Agrupamento de Materiais Inorgânicos - DQ-AMI

(2) National Industrial Research Institute of Nagoya - NIRIN

(3) National Institute for Research in Inorganic Materials - NIRIM

**Abstract:** Sintering of fine commercial SiC powders has been comparatively investigated: two 6H( $\alpha$ )-type (Showa Denko and H.C. Stark) and one 3C( $\beta$ )-type (Ibidem). Chemical composition, particle size distribution, and BET specific surface area were analyzed. SiC powders were mixed with 0.4% B<sub>4</sub>C powder, phenol resin (equivalent to ~1.8% C) and PEG during 8h in a planetary mill with ethanol. Dried and granulated powders were CIPed at 200MPa and then sintered at normal pressure between 1950 and 2250°C for 30min. in a high temperature dilatometer with flowing Ar atmosphere. The amounts of 2H, 3C, 4H, 6H, and 15R SiC polytypes were determined using X-ray diffraction analysis and a data-fitting method. Microstructures of the specimens were observed by scanning electron microscopy. Showa Denko and Ibidem powders presented good sinterability, but Stark powder presented good sinterability only after increasing the milling time. Density of sintered bodies increased with sintering temperature from 1950°C, achieved a maximum plateau between ~2100 and 2200°C, and decreased at 2250°C. Shrinkage curve of 3C( $\beta$ )-SiC powder was steeper than 6H( $\alpha$ )-SiC powders. Showa Denko powder presented: i) around 90% of 6H polytype until 2200°C, that dropped to ~70% at 2250°C; and ii) 4H polytype that slowly increased until 2200°C and had a abruptly increasing at 2250°C from ~7% to around 22%. The main difference of Stark powder was higher 4H polytype content at lower temperatures, that resulted on more elongated grains than Showa Denko powder. The reason for this difference seems to be related with the higher aluminum impurity content on Stark powder. Ibidem powder presented typical elongated microstructures with mainly continuous decreasing of 3C polytype and increasing of 4H, 6H and 15R polytypes with increasing sintering temperature.

**Key words:** silicon carbide; additives; polytypes; grain growth.

## Introduction

Silicon carbide (SiC) ceramics are being used in industry because they have several favorable properties, such as high elastic modulus and hardness, good thermal and chemical stability, low thermal and electrical conductivities, and relatively low thermal expansion coefficients. More applications include, for example, mechanical seals for liquid pumps and annealing furnaces for integrated-circuit (IC) wafers. From an industrial standpoint, SiC materials are classified as either  $\alpha$ -type phase (6H and noncubic phases) or  $\beta$ -type phase (cubic 3C).

SiC is a highly covalent bonded material and in the actual days the production of sintered products with high densities cannot be achieved without the use of sintering additives. Pressureless sintering of  $\beta$ -SiC with B and C, probably in the solid state, was first announced by Prochazka in 1975<sup>(1)</sup>. He proposed that C acts as a deoxidizing agent (reducing SiO<sub>2</sub> presented at the surface of SiC particles) and dissolved B segregates to grain boundaries and increases the atom diffusivity. The first would rise the interfacial energy and the second would decrease the grain boundary energy, both favoring the densification during the sintering of SiC.

Since of this work, many developments and advancing in acknowledgements on pressureless sintering of SiC have been made. New additives, optimization of additive contents, the way that they are introduced, atmosphere, the acknowledgements about polytype stability and the importance of carbon in solution are some examples<sup>(2-5)</sup>.

Others additive systems based on B-C have been developed, being the system B-C-Al the most prominent. The benefits of adding Al atoms are: i) to decrease the sintering temperature, probably assisted by the presence of a liquid phase even in the absence of oxygen; and ii) to generate a more elongated and interlocked grain structure by favoring the transformation of 6H to 4H polytype, that tends to increase the fracture toughness of SiC<sup>(6)</sup>.

Liquid phase sintering with oxide additives, like Al<sub>2</sub>O<sub>3</sub> and Y<sub>2</sub>O<sub>3</sub>, has been extensively studied mainly to lower the sintering temperature. In these systems the microstructure of SiC have been controlled by the addition of seeds that promote the formation of elongated grains in a equiaxed grain matrix<sup>(7-8)</sup>. A problem associated with oxide additive systems is the high mass loss during normal sintering (due to the formation of volatile SiO and CO gases) that difficult the complete densification of SiC<sup>(9)</sup>.

The aim of this study is to investigate the densification behavior of three kinds of fine commercial SiC powders by dilatometry. The difference in the densification behavior, density

and microstructure of sintered materials were correlated to the powder characteristics ( $\alpha$  or  $\beta$ -type and impurity level) and, in one case, to the milling time.

### Experimental procedure

Three types of industrially synthesized fine SiC powders were used in this study: two 6H( $\alpha$ )-type (Showa Denko Co., Tokyo, Japan, *DU A-1*, and H.C. Stark, GmbH & Co., KG, Postfach 2540, D-38615 Goslar, *UF-15*, hereinafter  $\infty$ -1 and  $\infty$ -2, respectively) and one 3C( $\beta$ )-type (Ibidem Co., Gifu, Japan, *Betarundum Ultrafine Grade*, hereinafter  $\beta$ ). The powders were analyzed via chemical analysis (free carbon, free SiO<sub>2</sub>, aluminum and iron), in accordance with Japanese Industrial Standard (JIS) R-1616. The particle size distributions by laser scattering method and BET specific surface areas of these powders were also determined.

Each SiC powder was wet mixed in ethanol with 0.4wt% B<sub>4</sub>C powder (Cerac), phenolic resin (5% over the total mass, that yielded after decomposition the equivalent of ~1.8% C) and polyethylene glycol (PEG) (2% over the total mass) during 8h in a planetary mill, with SiC milling media to avoid contamination. Only powder  $\infty$ -2 (H.C. Stark) was further 100h milled to improve sinterability. Dried and granulated powders were CIPed at 200MPa to prepare green bodies with approximately 5x6x20mm<sup>3</sup>. The samples were sintered in two stages in a high temperature dilatometer (Netsch 402 E/7, Selb Germany) with graphite crucible: first they were heat-treated under vacuum at 1500°C for 30min. (minimum pressure of ~10<sup>-1</sup>Pa), and then sintered at normal pressure between 1950 and 2250°C for 30min. with flowing Ar atmosphere (heating rate of 8°C/min.).

The density of green bodies and some low density sintered samples was determined by mass and dimensions measurements, and the density of the rest of sintered samples was determined by liquid (water) immersion method (Archimedean Principle). The sintered samples were surface polished until 1 $\mu$ m diamond. The amounts of 2H, 3C, 4H, 6H, and 15R SiC polytypes were determined using X-ray diffraction analysis and a data-fitting method proposed by one of the authors<sup>(10)</sup>. The microstructure of the polished and chemically etched surface (boiling method with Murakami's reagent, a saturated solution of equal parts of NaOH and K<sub>3</sub>Fe(CN)<sub>6</sub>) of each specimen was observed by optical microscopy and scanning electron microscopy.

## Results and discussion

The characteristics of SiC powders are presented in Table I. Powders  $\alpha$ -1 and  $\alpha$ -2 presented almost the same levels of free carbon and iron impurities, but powder  $\alpha$ -2 presented higher contents of free silica and aluminum impurities; both powders were constituted mainly by non-cubic polytypes (predominantly 6H). Powder  $\beta$ , in comparison with 6H( $\alpha$ ) powders, presented higher contents of free carbon and aluminum and was constituted mainly by cubic 3C polytype. Concerning to the granulometry, powder  $\alpha$ -1 presented larger average particle size and broader, probably bimodal, particle size distribution. Although powders  $\alpha$ -2 and  $\beta$  presented almost the same particle size distribution, powder  $\beta$  presented higher surface area. Figure 1 presents the SEM pictures of the three powders studied. Powder  $\alpha$ -2 (Figure 1b) presented particles with sharp or angular morphology and smooth cleaved surfaces, indicative of intense comminution during powder preparation.

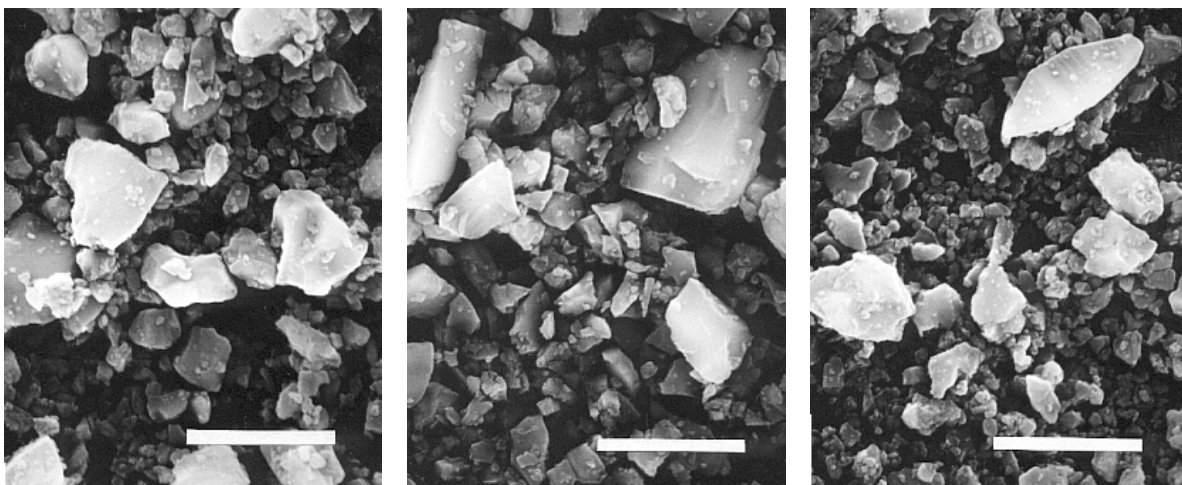
Table I: Powder characteristics.

Powder	Chemical analysis (mass %)				Polytype content (%)					Particle size ( $\mu\text{m}$ )			S ( $\text{m}^2/\text{g}$ )
	Free C	Free $\text{SiO}_2$	Fe	Al	2H	3C	4H	6H	15R	D <sub>10</sub>	D <sub>50</sub>	D <sub>90</sub>	
$\alpha$ -1*	0.49	0.34	0.030	0.004	0	2	0	91	7	0.34	0.71	2.33	13.3
$\alpha$ -2**	0.30	0.92	0.026	0.016	2	5	1	85	7	0.34	0.53	0.94	14.6
$\beta$ ***	0.81	0.37	0.035	0.044	5	94	0	0	1	0.34	0.50	0.93	19.1

Notes: \* - Showa Denko (DU A-1); \*\* - H.C. Stark (UF-15);

\*\*\* - Ibidem (Betarundum Ultrafine Grade);

S – specific surface area (BET method).



(a)  $\alpha$ -1

(b)  $\alpha$ -2

(c)  $\beta$

Figure 1: SEM images of powders  $\alpha$ -1,  $\alpha$ -2 and  $\beta$ . (Bar = 2.0 $\mu\text{m}$ .)

Green densities of powders  $\alpha$ -1,  $\alpha$ -2 and  $\beta$  were  $\sim 65\%$ TD (theoretical density),  $\sim 55\%$ TD and  $\sim 60\%$ TD, respectively. Probably the better compaction of powder  $\alpha$ -1 is related with its larger and broader particle size distribution; on the otherwise the worst compaction of powder  $\alpha$ -2 seems to be related with its narrow particle size distribution and angular morphology. Increasing the milling time of powder  $\alpha$ -2 caused no appreciable change on the particle size distribution, neither on the green density.

Figure 2 presents the shrinkage curves of sample  $\beta$  sintered at different holding temperatures. The maximum shrinkage attained during heating (without considering holding time) was  $2150^{\circ}\text{C}$ . Similar results were observed on shrinkage curves of sample  $\alpha$ -1. The first stage of sintering ( $1500^{\circ}\text{C}$ , 30min., vacuum) caused almost no shrinkage on all samples.

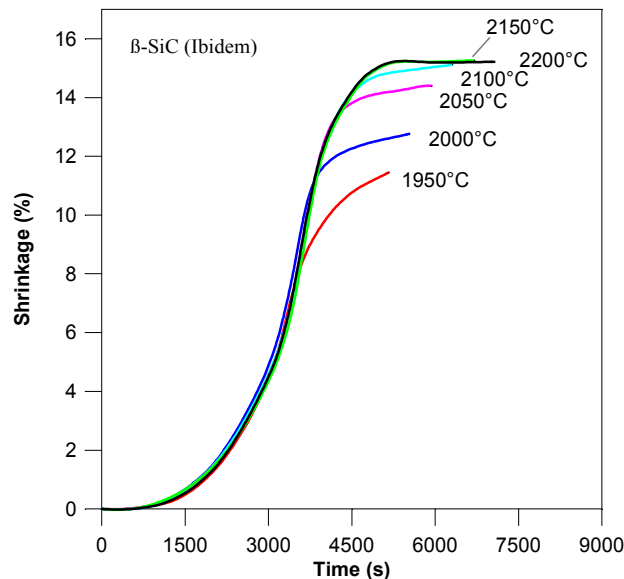


Figure 2: Shrinkage curves of sample  $\beta$  sintered at different holding temperatures.

Figure 3 presents the results of densification curves (estimated from shrinkage data) and shrinkage rate curves of samples  $\alpha$ -1,  $\alpha$ -2,  $\alpha$ -2 milled 100h, and  $\beta$  sintered at  $2150^{\circ}\text{C}$ . Sample  $\alpha$ -2 presented low densification when the same powder preparation procedure, employed to samples  $\alpha$ -1 and  $\beta$ , was used. Further 100h milling of powder  $\alpha$ -2 improved its sinterability, and sample with density comparable to samples  $\alpha$ -1 and  $\beta$  was obtained (Figure 3a). Although all samples presented significant shrinkage mainly between around  $1650$  and  $2150^{\circ}\text{C}$ , the temperature of maximum shrinkage rate varied among samples (Table II).

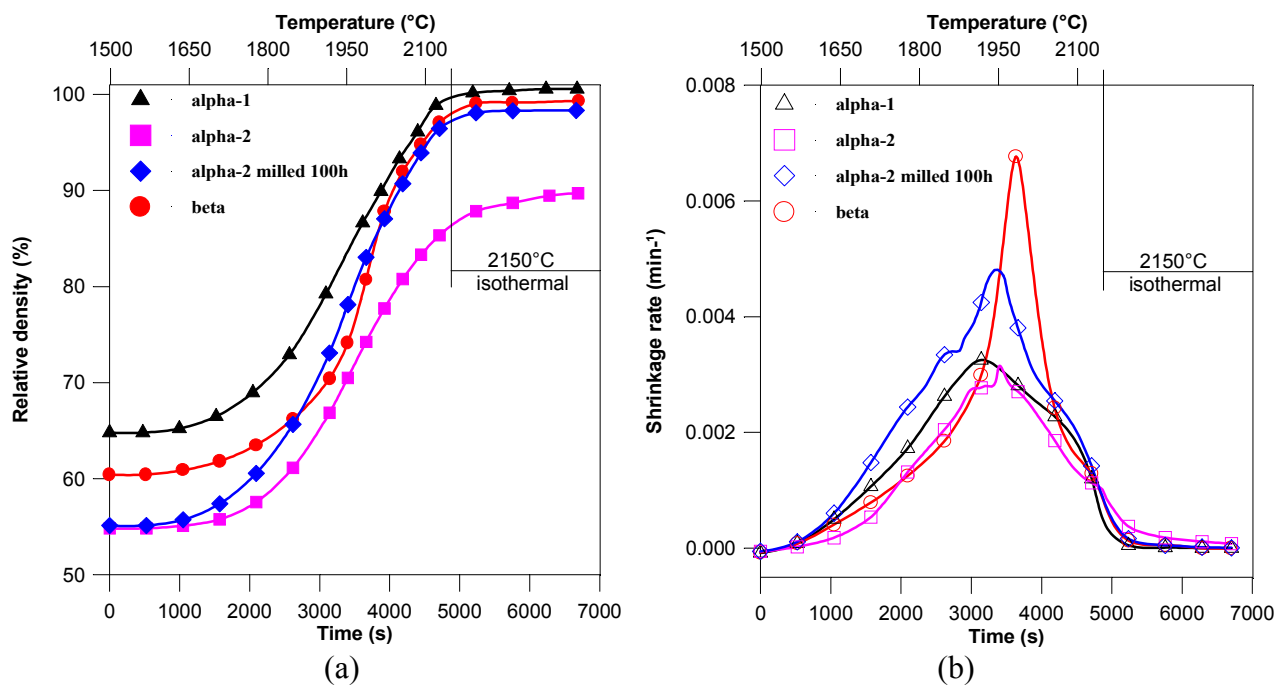


Figure 3: Relative density (a) and shrinkage rate (b) as a function of sintering time of samples  $\alpha$ -1,  $\alpha$ -2,  $\alpha$ -2 milled 100h, and  $\beta$ .

Table II: Temperature of maximum shrinkage rate.

$\alpha$ -1	$\alpha$ -2	$\alpha$ -2 milled 100h	$\beta$
1915°C	1940°C	1930°C	1980°C

The improvement on sinterability of powder  $\alpha$ -2 by milling was accomplished by an increase on shrinkage rate (Figure 3b) with almost no shifting on the peak temperature (Table II). Although powder  $\alpha$ -2 had, compared to powder  $\alpha$ -1, lower average particle size, narrower particle size distribution and higher specific surface area (Table I), it presented poor sinterability. The low green density of this powder could have contributed to this low performance. After 100h milling, powder  $\alpha$ -2 presented good sinterability, without apparently changing its particle size distribution and density of green compact. Another reason for poor sinterability of powder  $\alpha$ -2 can be related with its higher content of silica impurity than powder  $\alpha$ -1 (Table I). In a previous work <sup>(11)</sup> it was observed that 6H-SiC powders that contained the most silica impurity required the greatest amount of boron additive for complete densification, since silica seems to react with boron, reducing its effect on sintering. The benefic effect of milling on the improvement of powder  $\alpha$ -2 sinterability is not clear. One possibility could be an increase on homogeneity of additive distribution, that could increase the effectiveness of additives.

The main difference on densification behavior among powders  $\alpha$ -1,  $\alpha$ -2 milled 100h and  $\beta$  was the narrower shrinkage rate curve of powder  $\beta$ , with its maximum shifted to higher temperature (Figure 3b and Table II). This result indicates that more care on heating cycle of 3C( $\beta$ ) powders should be necessary on sintering of thick bodies.

Figure 4 presents bulk densities of samples sintered for 30min. between 1950 and 2250°C. The density of samples  $\alpha$ -1 and  $\beta$  steadily increased with increasing temperature until around 2100°C, remained almost constant until around 2200°C, and at 2250°C presented a small drop of around one percent. In a given temperature sample  $\alpha$ -1 presented higher density than sample  $\beta$ , the difference varying between 0.4 and 1.3% in the range of 2000 to 2250°C (at 1950°C the difference was ~3.0%). The highest densities determined for samples  $\alpha$ -1,  $\alpha$ -2 milled 100h and  $\beta$  were 3.184g/cm<sup>3</sup> (99.2%TD), 3.168g/cm<sup>3</sup> (98.7%TD) and 3.161g/cm<sup>3</sup> (98.5%TD), respectively (all sintered at 2150°C). Sample  $\alpha$ -2, without further milling, presented low density even sintered at 2200°C (Figure 4).

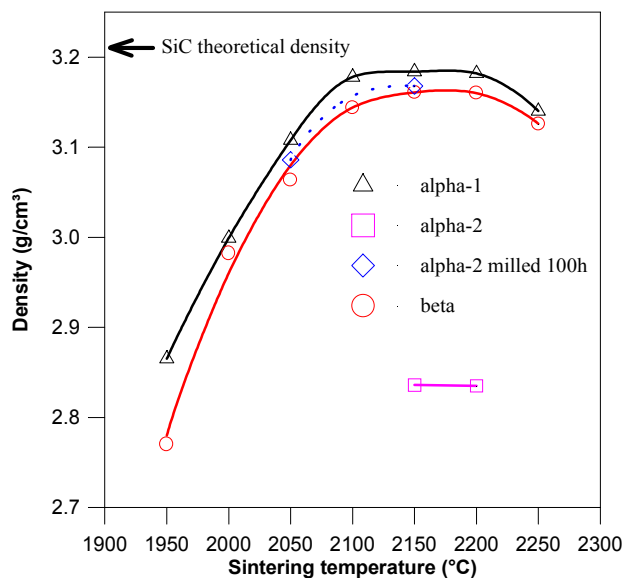


Figure 4: Bulk densities of samples  $\alpha$ -1,  $\alpha$ -2,  $\alpha$ -2 milled 100h, and  $\beta$  sintered for 30min. between 1950 and 2250°C.

Figure 5 shows polytype content as a function of sintering temperature (as reference, results of starting powders are also indicated). Sample  $\alpha$ -1 presented until 2200°C ~90% of 6H polytype and a slow increase of 4H polytype content; at 2250°C 6H content dropped to ~70% and 4H content abruptly increased to ~22% (Figure 5a). Around 5% of 15R polytype and some traces of 2H and 3C polytypes were also observed.

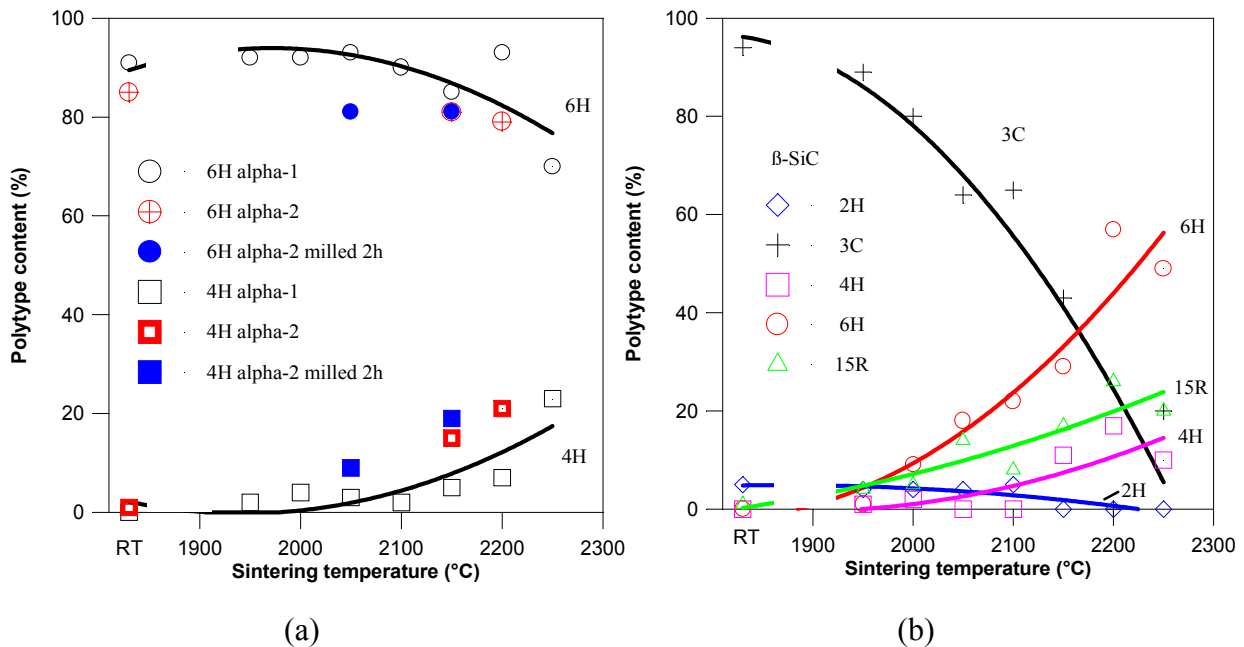


Figure 5: Polytype content as a function of sintering temperature of samples  $\alpha-1$ ,  $\alpha-2$ ,  $\alpha-2$  milled 100h (a) and sample  $\beta$  (b). (RT – room temperature.)

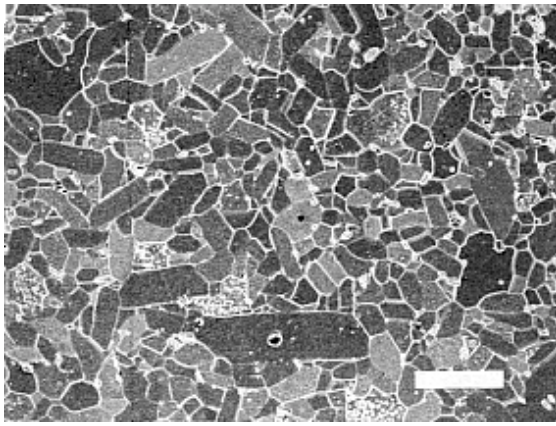
Samples  $\alpha-2$  and  $\alpha-2$  milled 100h presented slight lower 6H polytype content and higher 4H polytype content than sample  $\alpha-1$  (Figure 5a).

Sample  $\beta$  presented, between 1950 and 2250°C, strong decreasing of 3C polytype content (from ~90% to ~20%) and increasing of non-cubic polytypes, mainly 6H (from ~1% to ~50%), followed by 15R (from ~4% to ~20%) and 4H (from ~1% to ~10%). Some traces (around 5%) of 2H polytype were observed until 2100°C (Figure 5b).

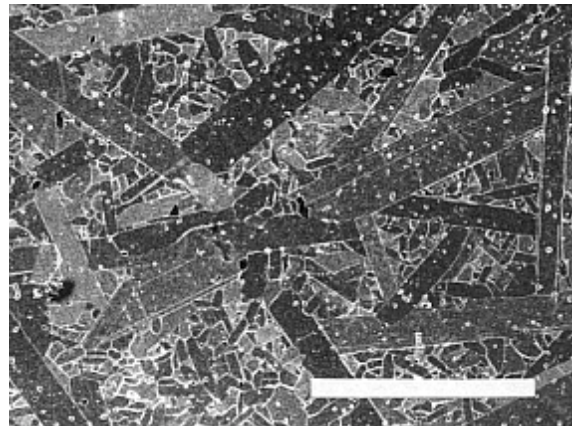
Comparing the polytype contents of samples  $\alpha-1$  and  $\beta$  between 1950 and 2250°C (Figure 5), it was observed that sample  $\alpha-1$  is more stable than sample  $\beta$  in relation to polytypic transformation.

Figure 6 presents some micrographs of sintered samples. Sample  $\alpha-1$  presented until 2150°C a relatively homogeneous microstructure with grains of approximately equiaxed shape (Figure 6a). At 2200°C abnormal grain growth resulted in a bimodal grain size distribution with large platelike grain (Figure 6b), and at 2250°C a coarse microstructure having predominantly large platelike grains was observed. Abnormal grain growth occurred simultaneously with the phase transformation of 6H to 4H polytype (Figure 5a).

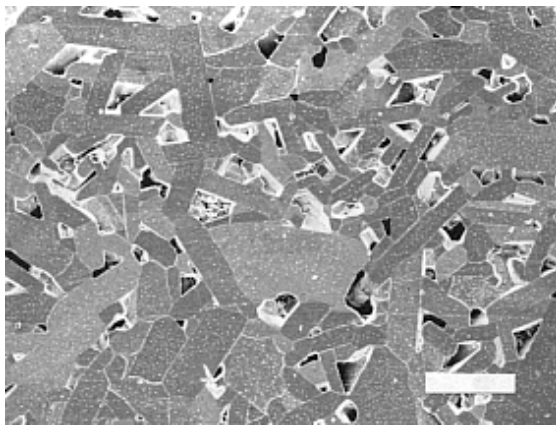




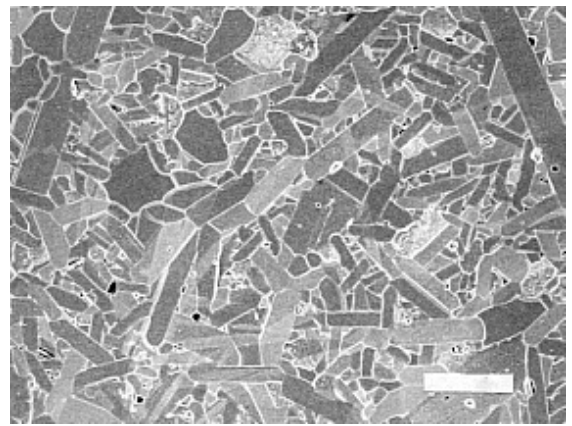
(a)  $\alpha$ -1 - 2150°C



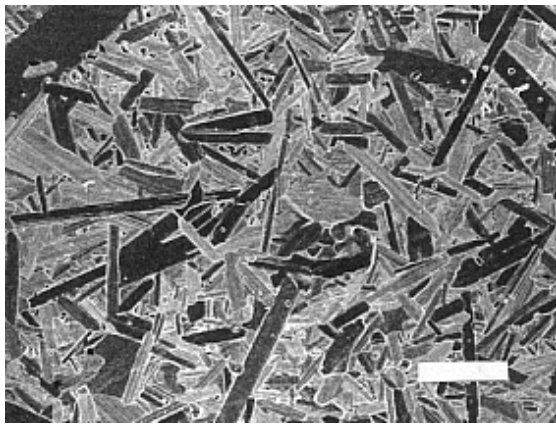
(b)  $\alpha$ -1 - 2200°C



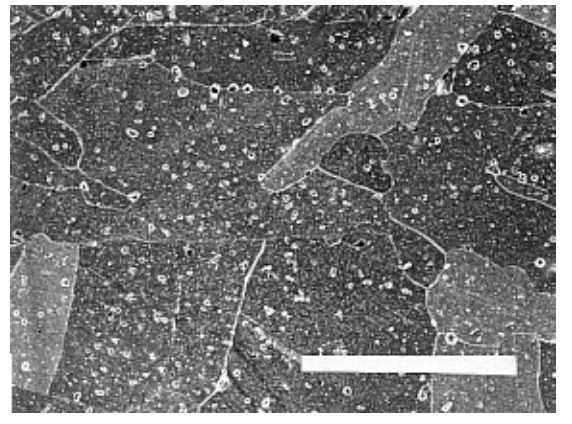
(c)  $\alpha$ -2 - 2150°C



(d)  $\alpha$ -2 milled 100h - 2150°C



(e)  $\beta$  - 2150°C



(f)  $\beta$  - 2200°C

Figure 6: SEM of the chemically etched surfaces: (a)  $\alpha$ -1 sintered at 2150°C; (b)  $\alpha$ -1 sintered at 2200°C; (c)  $\alpha$ -2 sintered at 2150°C; (d)  $\alpha$ -2 milled 100h sintered at 2150°C; (e)  $\beta$  sintered at 2150°C; (f)  $\beta$  sintered at 2200°C. (Bar = 10 $\mu$ m at a, c, d, e, and = 60 $\mu$ m at b, f.)

Sample  $\alpha$ -2 sintered at 2150 and 2200°C presented elongated grains with large pores, generally located at grain boundaries (Figure 6c). Sample  $\alpha$ -2 milled 100h sintered at 2150°C presented low porosity and a microstructure constituted mainly by elongated grains with some large platelike grains (Figure 6d). Sample  $\alpha$ -2 that did not densify enough showed larger grain growth than the milled  $\alpha$ -2.

Sample  $\beta$  presented, between 1950 and 2150°C, relative homogeneous microstructures containing elongated grains with some large platelike grains (Figure 6e). At 2200 and 2250°C the microstructure changed dramatically to one containing very large irregular grains (Figure 6f). The transformed  $\beta$ -SiC (3C to 6H, 15R and 4H, Figure 5b) seemed to be faulty, having many stacking faults, that could be observed in SEM analysis. This result indicated that the partial transformation or stacking faults in transformed 3C SiC made the SiC grains elongate.

In general, samples with good sinterability ( $\alpha$ -1,  $\alpha$ -2 milled 100h and  $\beta$ ) presented relative homogeneous microstructures with normal grain growth until 2150°C, when maximum densification was achieved. Above this temperature, abnormal grain growth occurred resulting on coarse microstructures (Figure 6).

The results showed that SiC powders, with good sinterability, sintered with B and C additives between 1950 and 2250°C presented similar densification behavior (Figure 4) and similar tendency to the occurrence of abnormal grain growth, irrespective of polytypic nature of starting powder.

Until 2150°C sample  $\alpha$ -2 presented microstructure with more elongated grains than sample  $\alpha$ -1 (Figure 6a, 6c and 6d). This seems to be related with higher content of aluminum impurity on starting powder  $\alpha$ -2 compared with powder  $\alpha$ -1 (Table I). In a previous work <sup>(11)</sup> it was observed that 6H-SiC powder that contained the highest level of aluminum impurity exhibited partial transformation of 6H to 4H polytype that seems to have induced elongated grain growth. Aluminum atoms are thought to have stabilized 4H polytype and accelerated the transformation of 6H polytype during sintering. The higher content of 4H polytype on sample  $\alpha$ -2 compared with sample  $\alpha$ -1 can be seen in Figure 5a. Starting powder  $\alpha$ -2 presented small amounts of 2H, 3C and 4H (Table I). It is possible that these polytype impurities acted as embryos for transformation at high temperature where transformation began.

## Summary

Three fine commercial SiC powders, two 6H( $\alpha$ )-type (Showa Denko DU A-1 and H.C. Stark UF-15, named  $\alpha$ -1 and  $\alpha$ -2, respectively) and one 3C( $\beta$ )-type (Ibidem UF, named  $\beta$ ), were pressureless sintered with 0.4% B<sub>4</sub>C and ~1.8% C between 1950 and 2250°C in a high temperature dilatometer with flowing Ar atmosphere. The great effect of milling on sintering was observed in powder  $\alpha$ -2, that presented good sinterability only after increasing the milling time. The main difference on densification behavior among powders was the narrower shrinkage rate curve of powder  $\beta$ , with its maximum shifted to higher temperature. The grain growth and phase transformation simultaneously occurred. In  $\alpha$ -SiC, 6H tends to transform to 4H. Aluminum contamination favored the 6H to 4H transformation. The polytype impurities (2H, 3C and 4H) presented on powder  $\alpha$ -2 could have act as embryos for this transformation at high temperature and resulted on microstructure with more elongated grains. In  $\beta$ -SiC, 3C tends to partially transform to 6H, 15R and 4H. The transformed  $\beta$ -SiC seems to be faulty, having many stacking faults. Partial transformation or stacking faults in transformed 3C SiC made the SiC grains elongate.

## Acknowledgements

The authors thank Japan International Cooperation Agency-JICA for financial support for the research.

## References

1. S. Prochazka, Special Ceramics 6, British Ceram. Res. Assoc., 171-81 (1975).
2. H. Tanaka, in "Silicon Carbide Ceramics I" edited by S. Somiya and Y. Inomata, Elsevier 213-38 (1991).
3. R.M. William, B.N. Juterbock, C.R. Peters, T.J. Whalen, J. Am. Ceram. Soc., 67, C-62-64 (1984).
4. B.W. Kibbel and A.H. Heuer, J. Am. Ceram. Soc., 72, 517-19 (1989).
5. W. Bucker, H. Landfeemann, H. Hausner, Powder Metallurgy International, 13, 37-39 (1991).
6. Y. Zhou, H. Tanaka, S. Otani, Y. Bando, J. Am. Ceram. Soc., 82, 1959-64 (1999).
7. F.F. Lange, J. Mat. Sci., 10, 314-20 (1975).
8. N. Padture, J. Am. Ceram. Soc., 77, 519-23 (1994).

9. T. Grande, H. Sommerset, E. Hagen., K. Wiik, M.A. Einarsrud, J. Am. Ceram. Soc., 80, 1047-52 (1997).
10. H. Tanaka, N. Iyi, J. Am. Ceram. Soc., 78, 1223-29 (1995).
11. H. Tanaka, H.N. Yoshimura, S. Otani, Y. Zhou, M. Toriyama, J. Am. Ceram. Soc., 83, 226-28 (2000).